

Dynamical Complexity in Teleparallel Gauss- Bonnet Gravity

S. A. Kadam^{1,*}, Santosh V Lohakare^{1,†} and B. Mishra^{1,‡}

¹Department of Mathematics, Birla Institute of Technology and Science-Pilani, Hyderabad Campus, Hyderabad-500078, India

Abstract: The stable critical points and their corresponding cosmology are derived in the teleparallel gravity with an added Gauss-Bonnet topological invariant term. We have analyzed the dynamics of the Universe by presenting two cosmological viable models, showing the potential to describe different phases of the evolution of the Universe. The value of the deceleration parameter (q), total equation of state parameter (ω_{tot}) and dark energy equation of state parameter (ω_{DE}) have been presented against each critical point. The existence and stability conditions are also presented. We study the behavior of the phase space trajectories at each critical point. Finally, the evolutionary behavior of the deceleration parameter and the equation of state parameters have been assessed with the initial condition of the dynamical variables, and compatibility has been observed in connection with the present cosmological scenario.

Keywords: Teleparallel gravity, Gauss-Bonnet invariant, Dynamical system analysis, Phase portrait.

I. INTRODUCTION

The discovery of an accelerated expansion of the Universe has been confirmed by multiple cosmological observations [1, 2]. Post-discovery, there has been a significant amount of attention to the modified theories of gravity. The source responsible for this cosmic acceleration is an unidentified repulsive form of energy known as dark energy (DE) [3, 4]. To explain the nature of DE along with dark matter (DM) [5, 6] and inflation [7], researchers have attempted modifications to general relativity (GR). We know that it is possible to define a large number of connections in a manifold, and one of such connections is the Levi-Civita connection [8, 9], which is used to construct GR. This Levi-Civita connection is based on the assumptions of torsion-free, metric compatibility, and the assumption of curvature free. The assumption of curvature-free leads to the teleparallel theory of gravity. In the construction of this theory, the Weitzenböck connection [10, 11] is used, which is different from the Levi-Civita connection. Teleparallel gravity (TG) is an equivalent formulation of GR in which torsion rather than curvature is responsible for the gravitational interaction [12, 13]. The TG is considered as a gauge theory, whereas GR is a geometric theory [13, 14]. The same equations of motion apply to both the theory and the name Teleparallel Equivalent of General Relativity (TEGR) [11, 13, 15]. In a formulation like TEGR, the gravitational Lagrangian is referred to as the torsion scalar T and is derived from the contraction of the torsion tensor [16–18]. This is analogous to the Lagrangian of the GR, which is denoted by the curvature scalar R and is built from the contraction of the curvature tensor [14].

The simplest modification to GR is to generalize the action using an arbitrary function of the Ricci scalar, resulting in ghost-free $f(R)$ modified gravity [19–21]. In addition to this simple modification of GR, it is possible to construct action with higher curvature corrections, such as the Gauss-Bonnet combination G [22] and an arbitrary functions $f(G)$ [23, 24]. In teleparallel gravity, the Lagrangian takes the form of the torsion scalar T ; the equations are equivalent to general relativity. Teleparallel gravity replaces T with a generic function of torsion as $f(T)$ in TEGR, much as $f(R)$ gravity replaces R with $f(R)$ in Einstein-Hilbert general relativity. The modified TEGR is known as $f(T)$ gravity [25–27]. This modification extends the teleparallel Lagrangian T to an arbitrary function $f(T)$. Although TEGR and GR are equivalent at the level of evolution equations, $f(T)$ and $f(R)$ are not equivalent. The cosmological effects of $f(T)$ gravity are therefore novel and intriguing [28–31]. Inspired by the Gauss-Bonnet modification of GR in [32], a new generalization of the standard $f(T)$ gravity was proposed. This theory extends the function $f(T)$ to $f(T, T_G)$, where T_G is the Gauss-Bonnet topological invariant. In the teleparallel formalism, i.e. in $f(T, T_G)$ theory, all the degrees of freedom related to torsion are given and then completely extend the $f(T)$ gravity [33].

In this study, we have used the method of dynamical system analysis [34–38], which is an important tool in cosmology to qualitatively assess the behavior of solutions of the model rather than determining the analytical

* k.siddheshwar47@gmail.com

† lohakaresv@gmail.com

‡ bivu@hyderabad.bits-pilani.ac.in

solution from the complex equations [35]. This method examines the local asymptotic behavior of critical points of the dynamical system and then connects them to the primary cosmological epochs of the Universe. With this, one can also find a description of the overall dynamics of the Universe [39–41]. For instance, the radiation and matter-dominated eras correspond to saddle points, whereas a late-time DE domination corresponds to a stable critical point. However, the dependency on the selection of variables that characterize the solution is linked to the critical, which is one of the limitations of this approach. It is to be noted that the absence of any particular cosmological epoch of the Universe may not indicate the failure of the theory; rather, it is the failure of the associated dynamical system to demonstrate the presence of an epoch [37]. Although dynamical systems have been useful in revealing the main features of solutions in specific models, limited attempts have been made for a more systematic analysis of generic $f(T, T_G)$ cosmology [40]. Hence, our aim is to derive a general expression for a dynamical system that can explain the de Sitter, radiation-dominated, as well as cold dark matter-dominated fixed points.

The exact cosmological solutions in teleparallel Gauss-Bonnet extension theory, with the selection of cosmological viable models, are obtained in Ref. [33, 42]. The cosmological bouncing solutions are highlighted in the $f(T, T_G)$ formalism in Ref. [43]. In the $f(T, T_G)$ gravity formalism, the reconstruction of the cosmological model is studied in [44]. This theory also shows a confrontation with current observational data [45]. The dynamical system is analyzed, and the field equations of $f(T, T_G)$ gravity are presented in Ref. [40]. The same approach has been used to analyze the phases of evolution of the Universe in different teleparallel settings such as in $f(T)$ gravity [39], $f(T, \phi)$ gravity [46], $f(T, B)$ gravity [31, 34] and the other modified gravity theories [47, 48]. In this work, we shall analyze the evolution of the Universe through the dynamical system approach through the critical points and the behavior of the evolution parameters. The paper is organized as follows: We first start with an introduction to TG in Section II where we review the background properties up to $f(T, T_G)$ gravity. In Section III, we consider two forms of $f(T, T_G)$ has been considered Ref. [33]. Then, in Subsections III A and III B, we introduce the dynamical system analysis for the mixed power law model and the sum of the separated power law model, respectively. We summarize our results in Section IV and give our conclusion.

II. TELEPARALLEL GRAVITY

Instead of the Levi-Civita connection, which causes curvature in GR, the teleparallel connection [13] is used in TG. In GR, the curvature is a product of the Levi-Civita connection $\overset{\circ}{\Gamma}{}^\sigma{}_{\mu\nu}$ (Over-circles indicate quantities calculated using Levi-Civita connections throughout), which has been replaced by the teleparallel connection $\Gamma^\sigma{}_{\mu\nu}$ [10, 11]. In TG, the dynamical variables are the tetrad fields or the vierbein $e^A{}_\mu$, where $E_A{}^\mu$ is the inverse of $e^A{}_\mu$. The metric tensor $g_{\mu\nu}$ can be calculated from the tetrad fields as follows,

$$e^A{}_\mu e^B{}_\nu \eta_{AB} = g_{\mu\nu}, \quad E_A{}^\mu E_B{}^\nu g_{\mu\nu} = \eta_{AB}, \quad (1)$$

The Latin indices denote coordinates on the tangent space, and the Greek indices denote the indices on the general manifold [15]. Usually, tetrads also appear in the curvature-based gravity, but in most cases, these are suppressed [49]. This could be due to the fact that they are not flat in these settings, whereas in TG, they are introduced as flat connections. Another important feature of these tetrads is that they satisfy the orthogonality requirements,

$$e^A{}_\mu E_B{}^\mu = \delta_B^A, \quad e^A{}_\mu E_A{}^\nu = \delta_\mu^\nu. \quad (2)$$

The teleparallel (Weitzenböck) connection [12, 50] can be defined as,

$$E_A{}^\sigma \left(\partial_\mu e^A{}_\nu + \omega^A{}_{B\mu} e^B{}_\nu \right) := \Gamma^\sigma{}_{\nu\mu}, \quad (3)$$

The tetrad represents the degrees of freedom of the metric, while the spin connection $\omega^A{}_{B\mu}$ represents the six degrees of freedom of the local Lorentz invariance. So, the tetrad-spin connection pair makes equations of three-dimensional motion that include both the Lorentz and gravitational degrees of freedom. Given that the teleparallel Riemann tensor disappears, we define a torsion tensor by [10]

$$2\Gamma^\sigma{}_{[\nu\mu]} := T^\sigma{}_{\mu\nu}, \quad (4)$$

The torsion tensor is the measure of the antisymmetry of the connection [11], and the square bracket is the antisymmetry operator. We can also define a contortion tensor as,

$$\Gamma_{\mu\nu}^{\sigma} - \mathring{\Gamma}_{\mu\nu}^{\sigma} = \frac{1}{2} \left(T_{\mu}^{\sigma}{}_{\nu} + T_{\nu}^{\sigma}{}_{\mu} - T^{\sigma}{}_{\mu\nu} \right) := K^{\sigma}{}_{\mu\nu}, \quad (5)$$

which is directly related to the Levi-Civita connection and plays an important role in defining some scalars and relating curvature and torsional quantities. Using the torsion tensor, a torsion scalar can be defined as [11, 13, 15]

$$\frac{1}{4} T^{\alpha}{}_{\mu\nu} T^{\mu\nu}{}_{\alpha} + \frac{1}{2} T^{\alpha}{}_{\mu\nu} T^{\nu\mu}{}_{\alpha} - T^{\alpha}{}_{\mu\alpha} T^{\beta\mu}{}_{\beta} := T, \quad (6)$$

The action is based on the torsion scalar and will produce the same field equations as the Einstein-Hilbert action. Again, we mention that the Ricci scalar disappears when calculating with the teleparallel connection, so $R \equiv 0$. Here, we can define the standard Ricci scalar, $\mathring{R} = \mathring{R}(\mathring{\Gamma}^{\sigma}{}_{\mu\nu})$ [17, 18] as

$$\mathring{R} + T - B = R = 0. \quad (7)$$

B represents a total divergence term and is defined as

$$\frac{2}{e} \partial_{\rho} \left(e T^{\mu}{}_{\mu}{}^{\rho} \right) = B, \quad (8)$$

with $e = \det(e^a{}_{\mu}) = \sqrt{-g}$ is the determinant of the tetrad. The expression in Eq. (7) conclude that GR andTEGR produce equivalent field equations in the classical regime; hence, both are dynamically equivalent. Another interesting scalar invariant is the Gauss-Bonnet term [32, 36, 43–45, 51]

$$\mathring{R}^2 - 4\mathring{R}_{\mu\nu}\mathring{R}^{\mu\nu} + \mathring{R}_{\mu\nu\alpha\beta}\mathring{R}^{\mu\nu\alpha\beta} = G, \quad (9)$$

which has been derived in the TG setting and can be defined as

$$T_G = \left(K_a{}^i{}_e K_b{}^e{}_j K_c{}^j{}_f K_d{}^f{}_l - 2K_a{}^{ij} K_b{}^k{}_e K_c{}^e{}_f K_d{}^f{}_l + 2K_a{}^{ij} K_b{}^k{}_e K_f{}^{el} K_d{}^f{}_c + 2K_a{}^{ij} K_b{}^k{}_e K_{c,d}{}^{el} \right) \delta_{iklk}^{abcd} \quad (10)$$

where $\delta_{iklk}^{abcd} = \epsilon^{abcd} \epsilon_{ijkl}$ is the generalized Kronecker delta function [52]. This has equivalency with the regular Gauss-Bonnet term up to a total divergence term defined as follows,

$$\frac{1}{e} \delta_{ijkl}^{abcd} \partial_a \left[K_b{}^{ij} \left(K_c{}^k{}_d + K_d{}^m{}_c K_m{}^{kl} \right) \right] = B_G. \quad (11)$$

The T_G, B_G together produce the teleparallel equivalent of the Gauss-Bonnet term as

$$-T_G + B_G = G. \quad (12)$$

Similarly to the modifications of GR, we consider a generalization of the Einstein-Hilbert action by adding generalizations in terms of both the torsion scalar and the Gauss-Bonnet term. The Gauss-Bonnet term has been linked to both inflationary and dynamical aspects of DE. We, therefore, consider the action equation as [32, 36]

$$\mathcal{S}_{f(T, T_G)} = \frac{1}{2\kappa^2} \int d^4x e f(T, T_G) + \int d^4x e \mathcal{L}_m, \quad (13)$$

where $\kappa^2 = 8\pi G$, and \mathcal{L}_m is the matter Lagrangian in the Jordan frame.TEGR is recovered for the limit where $f(T, T_G) \rightarrow -T$. In this formalism, the second and fourth-order contributions to the field equations are associated with the torsion scalar and Gauss-Bonnet term contributions, respectively. For a spatially flat, homogeneous, and isotropic cosmological background, the tetrad can be written as [13]

$$e^A{}_{\mu} = \text{diag}(1, a(t), a(t), a(t)), \quad (14)$$

where $a(t)$ is the scale factor that produces the spatially flat homogeneous and isotropic metric

$$ds^2 = -dt^2 + a(t)^2(dx^2 + dy^2 + dz^2), \quad (15)$$

through Eq. (1). The tetrad in Eq. (14) is compatible with the Weitzenböck gauge where $\omega^A_{B\mu} = 0$ [50, 53]. Using the definitions in Eq. (6)–Eq. (10),

$$T = 6H^2, \quad T_G = 24H^2 (\dot{H} + H^2), \quad (16)$$

where the Gauss-Bonnet term turns out to have the same value for this background as its curvature analogue. The Friedmann equations for this set-up obtained to be [36, 52]

$$F - 12H^2 F_T - T_G F_{T_G} + 24H^3 \dot{F}_{T_G} = 2\kappa^2 \rho, \quad (17a)$$

$$F - 4(\dot{H} + 3H^2) F_T - 4H \dot{F}_T - T_G F_{T_G} + \frac{2}{3H} T_G \dot{F}_{T_G} + 8H^2 \ddot{F}_{T_G} = -2\kappa^2 p. \quad (17b)$$

An over-dot refers to derivatives with respect to cosmic time t . To establish the deviation of this theory from GR and to better probe the role from the modified Lagrangian, we consider $F(T, T_G) = -T + f(T, T_G)$. Subsequently, Eq. (17a)–Eq. (17b) reduce respectively as,

$$6H^2 + f - 12H^2 f_T - T_G f_{T_G} + 24H^3 \dot{f}_{T_G} = 2\kappa^2 \rho, \quad (18a)$$

$$2(2\dot{H} + 3H^2) + f - 4(\dot{H} + 3H^2) f_T - 4H \dot{f}_T - T_G f_{T_G} + \frac{2}{3H} T_G \dot{f}_{T_G} + 8H^2 \ddot{f}_{T_G} = -2\kappa^2 p. \quad (18b)$$

Now, the Friedmann equations (18a- 18b) become

$$3H^2 = \kappa^2 (\rho + p_{DE}), \quad (19a)$$

$$3H^2 + 2\dot{H} = -\kappa^2 (p + p_{DE}), \quad (19b)$$

from where the expressions for energy density and pressure for the DE sector can be retrieved as

$$\frac{-1}{2\kappa^2} (f - 12H^2 f_T - T_G f_{T_G} + 24H^3 \dot{f}_{T_G}) = \rho_{DE}, \quad (20a)$$

$$\frac{1}{2\kappa^2} (f - 4(\dot{H} + 3H^2) f_T - 4H \dot{f}_T - T_G f_{T_G} + \frac{2}{3H} T_G \dot{f}_{T_G} + 8H^2 \ddot{f}_{T_G}) = p_{DE}. \quad (20b)$$

These DE densities and pressure expressions will satisfy the continuity equation.

$$\dot{\rho}_{DE} + 3H (\rho_{DE} + p_{DE}) = 0 \quad (21)$$

III. DYNAMICAL SYSTEM ANALYSIS IN $f(T, T_G)$ GRAVITY

We shall first define the appropriate dynamical variables to analyze the dynamical system of higher-order teleparallel gravity [31, 34]. By differentiating the dynamical variables with respect to $N = \ln(a)$, the expressions for the autonomous dynamical system can be obtained and, subsequently, the critical points. We consider the Universe to be filled with two fluids, $\rho = \rho_m + \rho_r$, where ρ_m and ρ_r respectively are the energy density for matter and radiation phase. In the matter phase, the matter pressure $p_m = 0$ and therefore ω_m also vanishes. In the radiation phase, the EoS parameter, $\omega_r = \frac{1}{3}$. Therefore, with these considerations, we define the dynamical variables as follows

$$X = f_{T_G} H^2, \quad Y = \dot{f}_{T_G} H, \quad Z = \frac{\dot{H}}{H^2}, \quad V = \frac{\kappa^2 \rho_r}{3H^2}, \quad W = -\frac{f}{6H^2}. \quad (22)$$

The standard density parameters expressions for matter (Ω_m), radiation (Ω_r) and DE (Ω_{DE}) phase are respectively,

$$\Omega_m = \frac{\kappa^2 \rho_m}{3H^2}, \quad \Omega_r = \frac{\kappa^2 \rho_r}{3H^2}, \quad \Omega_{DE} = \frac{\kappa^2 \rho_{DE}}{3H^2}, \quad (23)$$

with

$$\Omega_m + \Omega_r + \Omega_{DE} = 1. \quad (24)$$

In terms of dynamical variables, we have,

$$\Omega_m + \Omega_r + W + 2f_T + 4XZ + 4X - 4Y = 1, \quad (25)$$

and

$$\Omega_{DE} = W + 2f_T + 4XZ + 4X - 4Y. \quad (26)$$

To express the autonomous dynamical system, we define the parameter $\lambda = \frac{\dot{H}}{H^3}$ [54], and so the general form of the dynamical system can be obtained by differentiating the dimensionless variables with respect to $N = \ln(a)$,

$$\begin{aligned} \frac{dX}{dN} &= 2XZ + Y, \\ \frac{dY}{dN} &= -\frac{3}{4} - (Z+2)Y - \frac{Z}{2} + \frac{3W}{4} + (Z+3)\frac{f_T}{2} + \frac{\dot{f}_T}{2H} + 3X(Z+1) - \frac{V}{4}, \\ \frac{dZ}{dN} &= \lambda - 2Z^2, \\ \frac{dW}{dN} &= -2f_T Z - 8XZ^2 - 4X\lambda - 16XZ - 2WZ, \\ \frac{dV}{dN} &= -4V - 2VZ. \end{aligned} \quad (27)$$

To form the autonomous dynamical system, we need a form for $f(T, T_G)$ in which the terms $f_T, \frac{\dot{f}_T}{H}$ can be written in terms of the dimensionless variables, which we shall discuss by considering two forms of $f(T, T_G)$ as two models.

A. Mixed Power Law Model

We consider the mixed power law form of $f(T, T_G)$ [33] as

$$f(T, T_G) = f_0 T_G^k T^m, \quad (28)$$

where f_0, m, k are the arbitrary constants, the GR limit can be recovered for vanishing index powers. The motivation to consider this form is to study the role parameter $\lambda = \frac{\dot{H}}{H^3}$ in its most general form. From (22) and (28), we can write $f_T = -mW$, and this will guarantee the autonomous dynamical system and the dynamical variable X becomes,

$$\begin{aligned} X &= f_{T_G} H^2 = f_0 k G^{k-1} T^m H^2 \\ &= \frac{kfH^2}{G} = \frac{kf}{24(\dot{H} + H^2)} = \frac{kf}{6H^2} \left(\frac{1}{4\left(\frac{\dot{H}}{H^2} + 1\right)} \right) = \frac{-Wk}{4(Z+1)}. \end{aligned} \quad (29)$$

The parameter X depends on W with the condition on $Z \neq -1$. This condition also guarantees $T_G = 24H^4(Z+1)$, i.e. the non-vanishing teleparallel Gauss-Bonnet term. The dynamical variable W can be rewritten as

$$W = -\frac{4X(Z+1)}{k} \quad (30)$$

From Eq. (30), an expression for Z can be obtained and its derivatives, we get

$$\lambda = \frac{1}{1-k} \left[2(Z+1)Z(m-2) + 2Z^2(k+1) + 4kZ - \frac{(Z+1)Y}{X} \right] \quad (31)$$

We will consider X, Y, Z, V as independent variables, W and λ as dependent variables and then inserting f_T and $\frac{\dot{f}_T}{H}$ in to the system (27), we obtain

$$\begin{aligned} \frac{dX}{dN} &= 2XZ + Y, \\ \frac{dY}{dN} &= -\frac{k^2(V - 12X(Z+1) + 4Y(Z+2) + 2Z+3)}{4(k-1)k} + \frac{-8X(Z+1)(m(Z-3)+3) + V + 2Z+3}{4(k-1)} \\ &\quad - \frac{4(2m-1)X(Z+1)(2mZ+3)}{4(k-1)k} + \frac{4Y(2m(Z+1)+Z+2)}{4(k-1)}, \\ \frac{dZ}{dN} &= \frac{(Z+1)(Y - 2XZ(2k+m-2))}{(k-1)X}, \\ \frac{dV}{dN} &= -4V - 2VZ. \end{aligned} \quad (32)$$

We get the DE density parameter and the EoS parameter, respectively, in dynamical variables as,

$$\Omega_{DE} = -4Y + \frac{4X(Z+1)(k+2m-1)}{k}, \quad (33a)$$

$$\omega_{DE} = \frac{-k(V+2Z+3)}{12(X(Z+1)(k+2m-1) - kY)}. \quad (33b)$$

The critical points of the dynamical system can be obtained by considering $\frac{dX}{dN} = 0$, $\frac{dY}{dN} = 0$, $\frac{dZ}{dN} = 0$, $\frac{dV}{dN} = 0$, and are obtained as in Table I,

Name of Critical Point	X	Y	Z	V	Exist for
$A_1 = (x_1, y_1, z_1, v_1)$	x_1	$4x_1$	-2	v_1	$v_1 - 4x_1 - 1 \neq 0, m = \frac{v_1 - 12x_1 - 1}{v_1 - 4x_1 - 1}, k = \frac{1-m_1}{2},$ $-v_1x_1 + 8x_1^2 + x_1 \neq 0$
$A_2 = (x_2, y_2, z_2, v_2)$	x_2	$3x_2$	$-\frac{3}{2}$	0	$8x_2 + 1 \neq 0, x_2 \neq 0, y_2 \neq 0,$ $k = \frac{1-m}{2}, m^2 - 1 \neq 0$
$A_3 = (x_3, y_3, z_3, v_3)$	$\frac{1}{4}$	0	0	0	$k^2 - k \neq 0, m = \frac{1}{2}$
$A_4 = (x_4, y_4, z_4, v_4)$	x_4	0	0	0	$4x_4 - 1 \neq 0, (2m-1)x_4(8x_4+1)(8mx_4-1) \neq 0,$ $k = -\frac{4(2mx_4-x_4)}{4x_4-1}.$
$A_5 = (x_5, y_5, z_5, v_5)$	x_5	y_5	$-\frac{y_5}{2x_5}$	0	$y_5(12x_5 - 2y_5 + 1)(3x_5 - y_5) \neq 0$ $m = \frac{4x_5 + 2y_5 + 1}{12x_5 - 2y_5 + 1}$ $k = \frac{1-m}{2}, m^2 - 1 \neq 0$

Table I: The critical points (Model-III A)

The stability properties of the critical points are put into groups: (i) stable node: all the eigenvalues are negative; (ii) unstable node: all the eigenvalues are positive; (iii) saddle-node: one, two, or three of the four eigenvalues are positive, and the remaining are negative; (iv) stable spiral node: The determinant of the Jacobian matrix is negative, and the real part of all the eigenvalues is negative. We have summarized the stability of all the critical points for Model III A in Table II. To identify the phase of evolution, the value of the deceleration parameter q and the EoS parameter ($\omega_{tot}, \omega_{DE}$) are presented, corresponding to each critical point.

C. P.	Stability Conditions	q	ω_{tot}	ω_{DE}
A_1	Unstable	1	$\frac{1}{3}$	$\frac{1}{3}$
A_2	Stable for $m_2 < -1 \wedge \frac{1-m_2}{6m_2-10} < x_2 \leq \frac{8m_2-8}{9m_2^2-48m_2+71}$ Otherwise Unstable	$\frac{1}{2}$	0	0
A_3	Stable for $\frac{1}{4} < k \leq \frac{13}{25}$	-1	-1	-1
A_4	Stable for $x_4 < -\frac{1}{6} \wedge \left(m \leq \frac{17x_4+2}{72x_4^2+24x_4+2} \vee m > \frac{4x_4+1}{12x_4+1} \right)$	-1	-1	-1
A_5	Stable for $(x_5 < 0 \wedge y_5 > 3x_5) \vee (x_5 > 0 \wedge y_5 < 3x_5)$	$-1 + \frac{y_5}{2x_5}$	$-1 + \frac{y_5}{3x_5}$	$-1 + \frac{y_5}{3x_5}$

Table II: Stability condition, deceleration and EoS parameter (Model III A)

C. P.	Evolution Eqs.	Universe phase	Ω_m	Ω_r	Ω_{DE}
A_1	$\dot{H} = -2H^2$	$a(t) = t_0(2t + c_2)^{\frac{1}{2}}$	0	v_1	$1 - v_1$
A_2	$\dot{H} = -\frac{3}{2}H^2$	$a(t) = t_0(\frac{3}{2}t + c_2)^{\frac{2}{3}}$	$\frac{2(3m-5)x_2}{m-1} + 1$	0	$\frac{2(5-3m)x_2}{m-1}$
A_3	$\dot{H} = 0$	$a(t) = t_0 e^{c_1 t}$	0	0	1
A_4	$\dot{H} = 0$	$a(t) = t_0 e^{c_1 t}$	0	0	1
A_5	$\dot{H} = -\frac{y_5}{2x_5}H^2$	$a(t) = t_0(\frac{y_5}{2x_5}t + c_2)^{\frac{2x_5}{y_5}}$	0	0	1

Table III: Phase of the Universe, density parameters (Model-III A)

The cosmological solutions for the corresponding evolution equation at each critical point, along with the standard density parameters ($\Omega_m, \Omega_{DE}, \Omega_r$) for Model III A are presented in Table III.

The eigenvalues for the Jacobian matrix of the dynamical system in Eq. (32) at each critical point are presented in Table IV.

C.P.	Eigenvalues
A_1	$\left\{ 0, 1, \frac{x_1(v_1-8x_1-1)-r}{2x_1(-v_1+8x_1+1)}, \frac{r+x_1(v_1-8x_1-1)}{2x_1(-v_1+8x_1+1)} \right\}$
A_2	$\left\{ 0, -1, -\frac{\sqrt{(m^2-1)x_2(m((9m-48)x_2-8)+71x_2+8)}}{4(m^2-1)x_2} - \frac{3}{4}, \frac{\sqrt{(m^2-1)x_2(m((9m-48)x_2-8)+71x_2+8)}}{4(m^2-1)x_2} - \frac{3}{4} \right\}$
A_3	$\left\{ -4, -3, \frac{-\sqrt{25k^2-38k+13}-3k+3}{2(k-1)}, \frac{\sqrt{25k^2-38k+13}-3k+3}{2(k-1)} \right\}$
A_4	$\left\{ -4, -3, -\frac{s}{2x_4(8mx_4-1)} - \frac{3}{2}, \frac{3x_4(1-8mx_4)+s}{2x_4(8mx_4-1)} \right\}$
A_5	$\left\{ 0, -\frac{4x_5-y_5}{x_5}, -\frac{-8x_5y_5+12x_5^2+y_5^2}{2x_5(2x_5-y_5)}, -\frac{-5x_5y_5+6x_5^2+y_5^2}{x_5(2x_5-y_5)} \right\}$

Table IV: Eigenvalues corresponding to each critical point (Model III A)

The r, s are as described in **Appendix–A** [Eq. (37)]. The description of each of the critical points is as follows,

Critical Point $A_1(Z = -2)$: The critical point A_1 represents radiation dominated era with $\omega_{tot} = \omega_{DE} = \frac{1}{3}$ and $q = 1$, it describes the standard radiation dominated era for $v_1 = 1$, where $\Omega_r = 1$ and $\Omega_m = 0, \Omega_{DE} = 0$. The Jacobian matrix has one of the eigenvalues positive 1 presented in Table IV; therefore, this critical point is not stable, showing saddle point behavior. From the 2-D phase space in Fig. 1, we can observe that phase space trajectories are moving away from the critical point, further confirming the saddle point behavior.

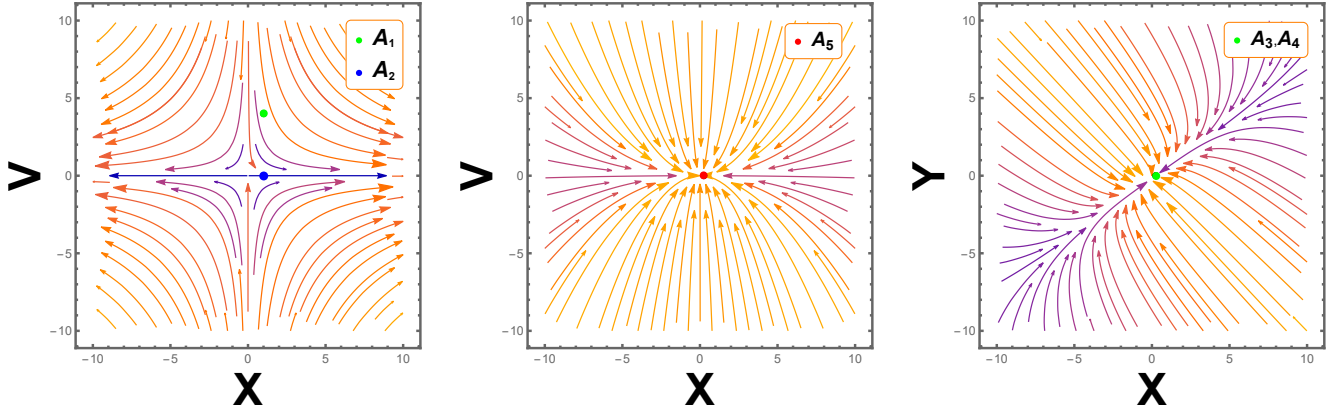


Figure 1: 2D phase portrait for the dynamical system of Model III A with $k = 0.029, m = 0.5$.

Critical Point $A_2(Z = -\frac{3}{2})$: The critical point A_2 describes a non-standard cold dark matter-dominated era with the negligible contribution of DE density $\Omega_{DE} = \frac{2(5-3m)x_2}{m-1}$. This critical point will represent a standard cold dark matter-dominated era for $x_2 = 0$ or $m = \frac{3}{5}$. The eigenvalues for the Jacobian matrix at this critical point are non-hyperbolic in nature, as presented in Table IV and show stability at the condition described in Table II. This critical point will either be a saddle or unstable node for the parameter range lying outside the stability condition described in II. We have plotted 2-D and 3-D phase portraits for $m = 0.5$, for which stability condition on x_2 is $-0.0714286 < x_2 \leq -0.0812183$. The coordinate of the phase portraits for 2-D and 3-D is in the unstable range for a critical point A_2 hence describing the saddle point nature of this critical point. The power law solution corresponding to the evolution equation at this critical point and the standard density parameters corresponding to different phases of the Universe evolution are presented in Table III. In this case, the values of $\omega_{tot} = \omega_{DE} = 0$, and the deceleration parameter will take the value $q = \frac{1}{2}$ which is positive; hence this critical point can not describe the current cosmic acceleration.

Critical Points $A_3, A_4(Z = 0)$: The critical points A_3 and A_4 both are the de-Sitter solutions with $\Omega_{DE} = 1, \Omega_m = 0, \Omega_r = 0$. The value of $\omega_{tot} = \omega_{DE} = q = -1$; hence these two critical points describe the current accelerated expansion of the Universe for all parametric values. The eigenvalues of the Jacobian matrix at both the critical points are presented in Table IV and are hyperbolic in nature and show stability at the stability conditions described in Table II. The phase space trajectories show attractor behavior, which can be assessed from Fig. 1.

Critical Point $A_5(Z \text{ depend on } Y, X)$: The value of the deceleration parameter, EoS parameters for this critical point is dependent on coordinates x and y as the value of $q = -1 + \frac{y_5}{2x_5}, \omega_{tot} = \omega_{DE} = -1 + \frac{y_5}{3x_5}$. This critical point represents a standard cold dark matter-dominated era with $\Omega_{DE} = 1$. This can explain the current cosmic acceleration at $(x_5 < 0 \wedge y_5 > 2x_5) \vee (x_5 > 0 \wedge y_5 < 2x_5)$. From the eigenvalues presented in Table IV, we can infer that the critical point is non-hyperbolic in nature and is stable at the stability condition presented in Table II. Since the phase space trajectories behavior can be analyzed from Fig. 1 are attracting towards the critical point A_5 , this critical point is an attractor.

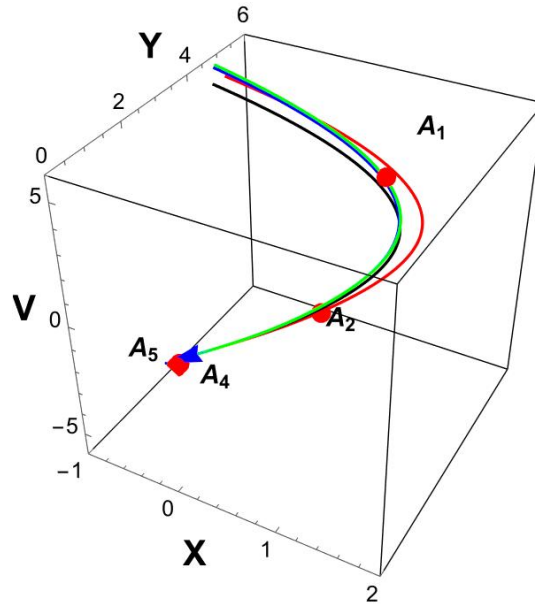


Figure 2: 3-D phase portrait for the Model III A with $k = 0.029, m = 0.5$.

The 3-D phase portrait presented in Fig. 2 allows us to analyze the behavior of trajectories at the critical points representing different phases of Universe evolution. Phase space trajectory passes through the critical point $A_1 \rightarrow A_2 \rightarrow A_4, A_5$. The 3D phase space trajectory can be seen in Fig. 2. We can see from the Figure that the chosen trajectory evolves from a radiation-dominant solution corresponding to critical point A_1 to an accelerating solution corresponding to critical points A_4 and A_5 . There may be first red dots in the trajectory transition between A_1 (radiation) and A_2 (matter) and last dots in the trajectory transition between A_4 and A_5 (de-sitter). Our final attractors, point A_4 and A_5 , represent the de-sitter epoch with cosmic acceleration.

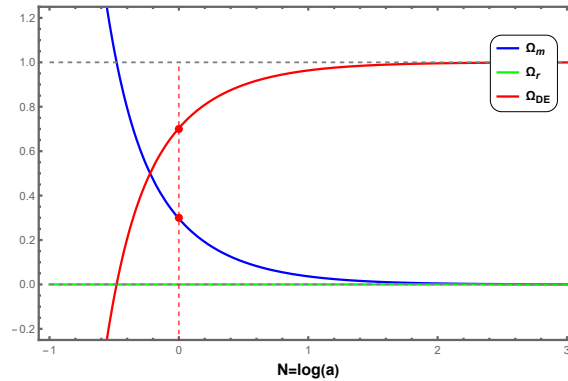


Figure 3: Evolution of the density parameters with initial conditions $X = -10^{-1}, Y = 10^{-5}, Z = 10^{-10}, V = 10^{-11}$, $k = 0.029, m = 0.5$ for Model III A.

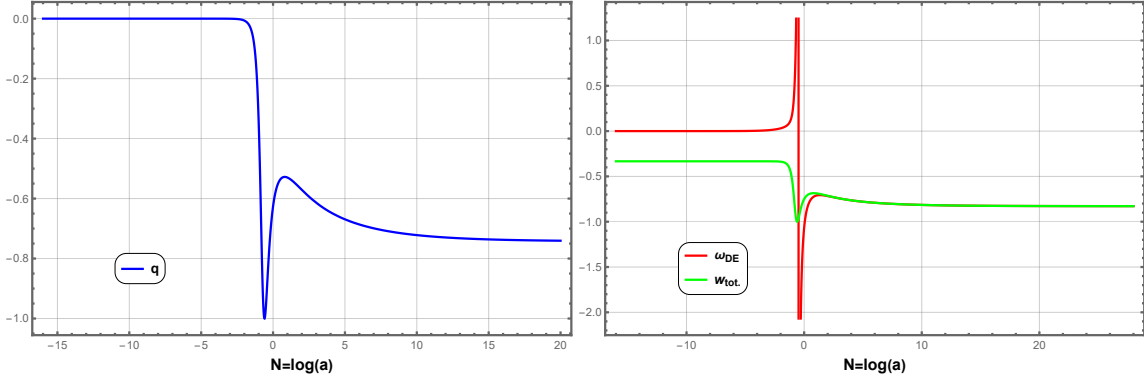


Figure 4: Deceleration and EoS parameter of Model III A. The initial conditions $X = -10^{-1}, Y = 10^{-5}, Z = 10^{-10}, V = 10^{-11}, k = 0.029, m = 0.5$.

The evolution plot for the standard density parameter is plotted in Fig. 3. The vertical dashed line represents a present time of cosmic evolution, at which the standard density parameter for matter and DE shows values approximately equal to 0.3 and 0.7, respectively. The value of the deceleration parameter at present time is $q_0 = -0.663$ which is compatible with the current observation study $q_0 = -0.528^{+0.092}_{-0.088}$ [55]. The plots for EoS parameters are presented in Fig. 4, from which we can study the early and late time evolution of the Universe. The present value of $\omega_{DE} = -1.05$ which is compatible with the WMAP+CMB [$\omega_0 = -1.073^{+0.090}_{-0.089}$] [56].

B. Sum of Separated Power Law Model

We consider the sum of the separated power law [33] form of $f(T, T_G)$ as

$$f(T, T_G) = g_0 T_G^k + t_0 T^m, \quad (34)$$

In this case, from the dynamical system variables defined in Eq. (22), we find $f_T = -mW - \frac{4m}{k}(1+Z)X$. The dynamical variable W can not be written as dependent on variables X and Z ; therefore, W has to be treated as an independent variable. We consider the dynamical variable $\lambda = \text{constant}$ in the further analysis of this model. By referring to the general dynamical system defined in Eq. (27), we can write the dynamical system in autonomous form as,

$$\begin{aligned} \frac{dX}{dN} &= 2XZ + Y, \\ \frac{dY}{dN} &= \frac{8m(X(\lambda + Z(2m(Z+1) + Z + 6) + 3) + YZ + Y)}{4k} - \left(\frac{(2m-1)(2mZ+3)W}{4} \right) \\ &\quad + \frac{1}{4}(-V - 4Y(Z+2) - 2Z - 3) + X(2\lambda m + Z(4m(Z+2) + 3) + 3), \\ \frac{dZ}{dN} &= \lambda - 2Z^2, \\ \frac{dV}{dN} &= -4V - 2VZ, \\ \frac{dW}{dN} &= \frac{8mXZ(Z+1)}{k} + 2(m-1)WZ - 4X(\lambda + 2Z(Z+2)). \end{aligned} \quad (35)$$

The density parameter and the EoS parameter for the DE can be written as,

$$\Omega_{DE} = \frac{4X(Z+1)(k-2m)}{k} - 2mW - 4Y + W, \quad (36a)$$

$$\omega_{DE} = \frac{k(-mWZ + V + 2Z + 3) - 4mXZ(Z+1)}{24mX(Z+1) - 3kD}. \quad (36b)$$

Here, $D = -2mW + 4X(Z + 1) - 4Y + W$. The critical points for the dynamical system in Eq. (35) with the existing condition are presented in Table V.

Name of Critical Points	X	Y	Z	V	W	Exist for
$B_1 = (X_1, Y_1, Z_1, V_1, W_1)$	0	0	-2	1	0	$k \neq 0, \lambda = 8, \text{arbitrary } m$
$B_2 = (X_2, Y_2, Z_2, V_2, W_2)$	X_2	$4X_2$	-2	V_2	W_2	$k = -\frac{4mX_2}{m(-V_2)+4mX_2+m+V_2-12X_2-1},$ $mV_2 - 4mX_2 - m - V_2 + 12X_2 + 1 \neq 0,$ $W_2 = V_2 - 4X_2 - 1,$ $\lambda = 8, mX_2 \neq 0.$
$B_3 = (X_3, Y_3, Z_3, V_3, W_3)$	0	0	-2	V_3	W_3	$W_3 = V_3 - 1 \neq 0, k \neq 0, m = 1, \lambda = 8$
$B_4 = (X_4, Y_4, Z_4, V_4, W_4)$	X_4	$4X_4$	-2	V_4	W_4	$X_4 \neq 0, V_4 = 12X_4 + 1,$ $W_4 = V_4 - 4X_4 - 1, k \neq 0.$ $\lambda = 8, m = 0.$
$B_5 = (X_5, Y_5, Z_5, V_5, W_5)$	0	0	$-\frac{3}{2}$	0	0	$k \neq 0, \lambda = \frac{9}{2}$
$B_6 = (X_6, Y_6, Z_6, V_6, W_6)$	0	0	$-\frac{3}{2}$	0	W_6	$W_6 \neq 0, k \neq 0, \lambda = \frac{9}{2}, m = \frac{3W_6 - 2W_6Z_6 - 2Z_6 - 3}{6W_6}$
$B_7 = (X_7, Y_7, Z_7, V_7, W_7)$	X_7	$3X_7$	$-\frac{3}{2}$	0	W_7	$-6mW_7 + 12X_7 - 12Y_7 + 3W_7 - 2W_7Z_7 - 2Z_7 - 3 \neq 0,$ $k = -\frac{12(2mX_7 - mY_7)}{6mW_7 - 12X_7 + 12Y_7 - 3W_7 + 2W_7Z_7 + 2Z_7 + 3},$ $2mX_7 - mY_7 \neq 0,$ $\lambda = \frac{9}{2}.$
$B_8 = (X_8, Y_8, Z_8, V_8, W_8)$	X_8	$3X_8$	$-\frac{3}{2}$	0	W_8	$X_8 \neq 0, W_8 = \frac{1}{3}(-12X_8 + 8Y_8 + 2Z_8 + 3),$ $k \neq 0, \lambda = \frac{9}{2}, m = 0$
$B_9 = (X_9, Y_9, Z_9, V_9, W_9)$	0	0	Z_9	0	-1	$Z_9(2Z_9 + 3) \neq 0, \lambda = 2Z_9^2, m = 1, k \neq 0$
$B_{10} = (X_{10}, Y_{10}, Z_{10}, V_{10}, W_{10})$	X_{10}	Y_{10}	$-\frac{Y_{10}}{2X_{10}}$	0	W_{10}	$X_{10} \neq 0, Y_{10}(3X_{10} - Y_{10}) \neq 0,$ $W_{10} = -12X_{10} + 2Y_{10} - 1,$ $12mX_{10} - 2mY_{10} + m - 4X_{10} - 2Y_{10} - 1 \neq 0,$ $k = \frac{2(2mX_{10} - mY_{10})}{12mX_{10} - 2mY_{10} + m - 4X_{10} - 2Y_{10} - 1}, \lambda = 2Z_{10}^2$ $2mX_{10} - mY_{10} \neq 0.$

Table V: The critical points (Model III B)

In this case, it can be noted that there are more critical points than in Model III A, also since λ is an independent variable, we can categorize the critical points for different phases of evolution on the basis of the value of λ . The system will describe radiation, matter, and the DE-dominated era for $\lambda = 8, \frac{9}{2}$, value depending on coordinates X and Y respectively. The stability conditions, the values of the deceleration parameter, $\omega_{DE}, \omega_{tot}$ at each critical point are presented in Table VI.

The evolution equations and the standard density parameters for radiation, matter, and DE at each critical point are presented in Table VII.

The stability of the critical points is obtained from the signature of the eigenvalues and is presented in Table VIII. The $\tau_i, i = 2, 5, 7, 9, 10$, in Table VIII are as described in Appendix-A [Eq. (38)].

The description for each critical point for the dynamical system in Eq-(35) is as follows,

Critical Points $B_1 - B_4, Z = -2, \lambda = 8$: In this case all the critical points $B_1 - B_4$ are describing the radiation-dominated era with the parametric value of $Z = -2, \lambda = 8$. The value of deceleration parameter $q = 1, \omega_{tot} = \frac{1}{3}$.

C. P.	Stability Conditions	q	ω_{tot}	ω_{DE}
B_1	Unstable	1	$\frac{1}{3}$	-
B_2	Unstable	1	$\frac{1}{3}$	$1 - \frac{8X_2}{V_2-1}$
B_3	Unstable	1	$\frac{1}{3}$	1
B_4	Unstable	1	$\frac{1}{3}$	$-\frac{4X_4}{V_4-24X_4-1}$
B_5	Unstable	$\frac{1}{2}$	0	-
B_6	Unstable	$\frac{1}{2}$	0	$\frac{1}{2}$
B_7	Unstable	$\frac{1}{2}$	0	$-\frac{5X_7}{6X_7+W_7} + \frac{1}{2}$
B_8	Unstable	$\frac{1}{2}$	0	0
B_9	Stable for $-\frac{3}{2} < Z_9 < -1 \wedge 4\sqrt{3}\sqrt{-\frac{Z_9^3+2Z_9^2+Z_9}{(25Z_9^2+22Z_9+1)^2}}$ $+\frac{2(5Z_9^2+6Z_9+1)}{25Z_9^2+22Z_9+1} \leq k < \frac{1}{2}$	$-1 - Z_9$	$-1 - \frac{2Z_9}{3}$	$-1 - Z_9$
B_{10}	Stable for $(\frac{1}{2} \leq m < 1 \wedge X_{10} < 0 \wedge Y_{10} > 0)$ $\vee (m > 1 \wedge X_{10} > 0 \wedge Y_{10} < 0)$	$-1 + \frac{Y_{10}}{2X_{10}}$	$-1 + \frac{Y_{10}}{3Y_{10}}$	$\frac{1}{6} \left(\frac{(2Y_{10}+3)Y_{10}}{Y_{10}} + 4Y_{10} - 6 \right)$

Table VI: Stability condition, deceleration and EoS parameter (Model III B)

C. P.	Evolution Eqs.	Universe phase	Ω_r	Ω_m	Ω_{DE}
B_1	$\dot{H} = -2H^2$	$a(t) = t_0(2t + c_2)^{\frac{1}{2}}$	1	0	0
B_2	$\dot{H} = -2H^2$	$a(t) = t_0(2t + c_2)^{\frac{1}{2}}$	V_2	0	$1 - V_2$
B_3	$\dot{H} = -2H^2$	$a(t) = t_0(2t + c_2)^{\frac{1}{2}}$	$1 + W_3$	0	$-W_3$
B_4	$\dot{H} = -2H^2$	$a(t) = t_0(2t + c_2)^{\frac{1}{2}}$	$12X_4 + 1$	$-V_4 + 12X_4 + 1$	$V_4 - 24X_4 - 1$
B_5	$\dot{H} = -\frac{3}{2}H^2$	$a(t) = t_0(\frac{3}{2}t + c_2)^{\frac{2}{3}}$	0	1	0
B_6	$\dot{H} = -\frac{3}{2}H^2$	$a(t) = t_0(\frac{3}{2}t + c_2)^{\frac{2}{3}}$	0	$1 + W_6$	$-W_6$
B_7	$\dot{H} = -\frac{3}{2}H^2$	$a(t) = t_0(\frac{3}{2}t + c_2)^{\frac{2}{3}}$	0	$6X_7 + W_7 + 1$	$-6X_7 - W_7$
B_8	$\dot{H} = -\frac{3}{2}H^2$	$a(t) = t_0(\frac{3}{2}t + c_2)^{\frac{2}{3}}$	0	$10X_8 + 1$	$-10X_8$
B_9	$\dot{H} = Z_9H^2$	$a(t) = t_0(-Z_9t + c_2)^{\frac{-1}{Z_9}}$	0	0	1
B_{10}	$\dot{H} = -\frac{Y_{10}}{2X_{10}}H^2$	$a(t) = t_0(\frac{Y_{10}}{2X_{10}}t + c_2)^{\frac{2X_{10}}{Y_{10}}}$	0	0	1

Table VII: Phase of the Universe, density parameters(Model-III B)

The value of ω_{DE} is undetermined at B_1 and $1 - \frac{8X_2}{V_2-1}, 1, -\frac{4X_4}{V_4-24X_4-1}$ for B_2, B_3, B_4 respectively. From Table VI, one can observe that all the critical points describing radiation dominated era are unstable. From Table VIII, in this case, the eigenvalues have zero as one of the eigenvalues; hence these critical points are non-hyperbolic in nature. Each critical point has at least one positive eigenvalue; hence, all critical points are unstable. The exact cosmological solution and the corresponding evolution equation are described in Table VII. The values of the standard density parameter imply that the critical point B_1 is the only critical point that defines a standard radiation-dominated era, and the other three critical points represent the non-standard radiation-dominated era in which a small amount of

C.P.	Eigenvalues
B_1	$\left\{ 0, 1, 8, -\frac{\sqrt{-4(2k+5)km+4(1-2k)^2m^2+49k^2}+2(2k-1)m+k}{2k}, \frac{\sqrt{-4(2k+5)kk+4(1-2k)^2m^2+49k^2}-k(4m+1)+2m}{2k} \right\}$
B_2	$\left\{ 0, 1, 8, \frac{(m-1)(V_2-1)X_2+2(5-6m)X_2^2-\tau_2}{4X_2^2}, \frac{(m-1)(V_2-1)X_2+2(5-6m)X_2^2+\tau_2}{4X_2^2} \right\}$
B_3	$\left\{ 0, 1, 8, -\frac{\sqrt{57k^2-36k+4}-5k+2}{2k}, \frac{\sqrt{57k^2-36k+4}-5k+2}{2k} \right\}$
B_4	$\{8, -4, 3, 1, 0\}$
B_5	$\left\{ 0, -1, 6, \frac{-12k^2m+4km-2k^2-\tau_5}{8k^2}, \frac{-12k^2\mu_3+4km-2k^2+\tau_5}{8k^2} \right\}$
B_6	$\left\{ 0, -1, 6, \frac{-7k^2+2k-\sqrt{97k^4-52k^3+4k^2}}{4k^2}, \frac{-7k^2+2k+\sqrt{97k^4-52k^3+4k^2}}{4k^2} \right\}$
B_7	$\left\{ 0, -1, 6, \frac{2mX_7W_7-12mX_7^2-\tau_7-2X_7W_7+6X_7^2}{8X_7^2}, \frac{2mX_7W_7-12mX_7^2+\tau_7-2X_7W_7+6X_7^2}{8X_7^2} \right\}$
B_8	$\left\{ 6, -3, \frac{5}{2}, -1, 0 \right\}$
B_9	$\left\{ -4Z_9, -2(Z_9+2), -2Z_9-3, \frac{1}{2} \left(-\frac{2(Z_9+1)}{k} + 3Z_9 - \frac{\tau_9}{k^2} + 1 \right), \frac{k(Z_9(3k-2)+k-2)+\tau_9}{2k^2} \right\}$
B_{10}	$\left\{ \frac{2Y_{10}}{X_{10}}, \frac{Y_{10}}{X_{10}} - 4, \frac{Y_{10}}{X_{10}} - 3, \frac{X_{10}(-m(12X_{10}+1)+6X_{10}+Y_{10}+1)-\tau_{10}}{4X_{10}^2}, \frac{X_{10}(-m(12X_{10}+1)+6X_{10}+Y_{10}+1)+\tau_{10}}{4X_{10}^2} \right\}$

Table VIII: Eigenvalues corresponding to each critical point(Model III B)

DE density contribute. The critical points B_2, B_3, B_4 will define a standard radiation-dominated era at the parametric values $V_2 = 1, W_3 = 0, X_4 = 0$, and $V_4 = 1$ respectively. The phase space trajectories near these critical points can be analyzed in Fig. 5. All the critical points representing the radiation-dominated era are plotted in a single plot. The phase space trajectories are moving away from all these critical points; hence we can analyze the saddle point behavior, which is unstable.

Critical Points B_5 - $B_8, Z = -\frac{3}{2}, \lambda = \frac{9}{2}$: These critical points are describing the cold-dark matter-dominated era. From Table VII, we can observe that the critical point B_5 represents the standard cold dark matter-dominated era and the other three B_6, B_7, B_8 critical points are representing the non-standard cold dark matter era. Again from Table VI, we see the value of $q = \frac{1}{2}$ and $\omega_{tot} = 0$ at all these critical points. The critical point B_6 represents the standard cold dark matter era at $W_6 = 0$ and similar to this, B_7 at $X_7 = 0, W_7 = 0$ and the critical point B_8 at $X_8 = 0$. From Table VIII, we observe that the eigenvalues are unstable, and the existence of one zero eigenvalues at each critical point implies that all the critical points are non-hyperbolic. The behavior of phase space trajectories can be analyzed from Fig. 5. The trajectories at these critical points are moving away from the critical points; hence, critical points show saddle point behavior.

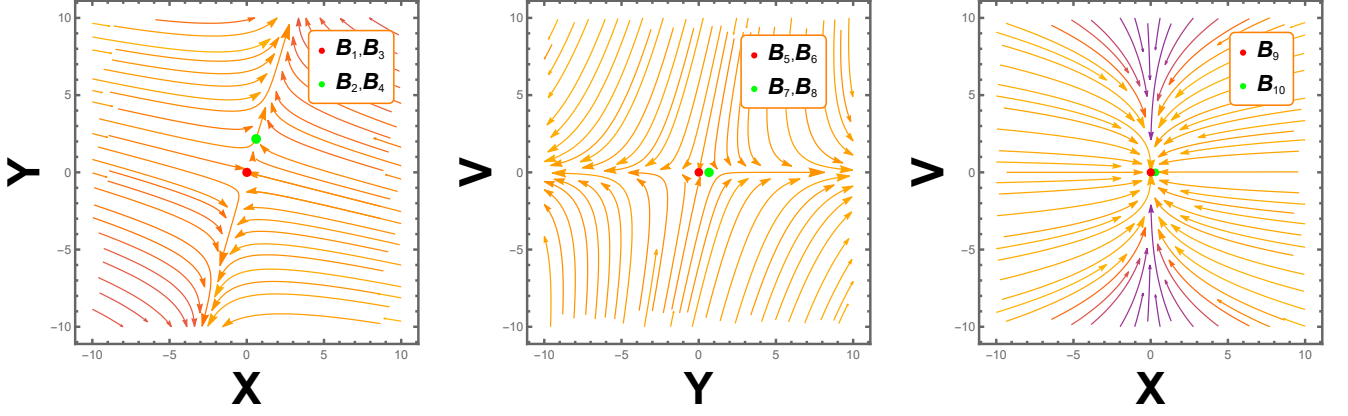


Figure 5: 2D phase portrait for the dynamical system of Model III B with $m = 0.61, k = 0.85$.

Critical Points B_9 - B_{10} , (λ, Z depend on X, Y): In these critical points, the value of parameter λ and Z are depending on co-ordinate X, Y , and Z . The critical points B_9 and at B_{10} may describe current cosmic acceleration, respectively, at $Z_9 > -1$ and $\left(Y_{10} \leq 0 \wedge \left(X_{10} < \frac{Y_{10}}{2} \vee X_{10} > 0 \right) \right) \vee \left(Y_{10} > 0 \wedge \left(X_{10} < 0 \vee X_{10} > \frac{Y_{10}}{2} \right) \right)$. The de-Sitter solution can be analyzed at $Z_9, Y_{10} = 0$ respectively for critical points B_9 and B_{10} . The hyperbolic or non-hyperbolic nature of these critical points depends on the coordinate values and shows stability at the conditions described in Table VIII. The exact cosmological solution and the evolution equations at these critical points are described in Table VII. From the behavior of phase space trajectories in Fig. 5, it can be observed that phase space trajectories are attracting towards both the critical points; hence, these critical points are attractors in behaviour.

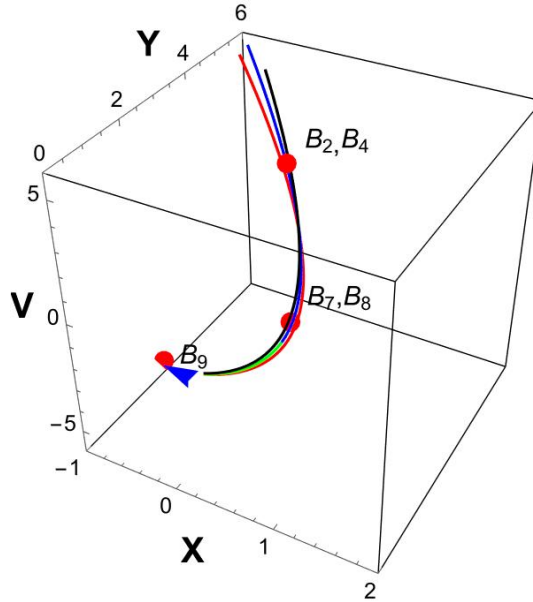


Figure 6: 3-D phase portrait for the (Model III B.) for $m = 0.61, k = 0.85$.

The trajectory plots show a path from the matter-dominated unstable critical points B_2 and B_4 to the stable dark energy-dominated critical point B_9 . This path is represented by the following sequence: $B_2, B_4 \rightarrow B_7, B_8 \rightarrow B_9$.

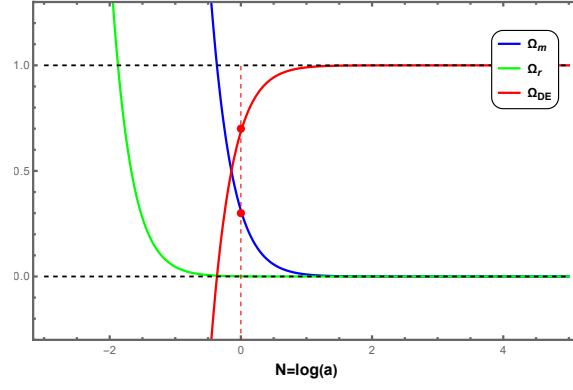


Figure 7: Evolution of the density parameters with initial conditions $X = -10^{-1.3}$, $Y = 0.089$, $Z = 0.02 \times 10^{-2}$, $V = 0.2 \times 10^{-1.5}$, $W = 0.021 \times 10^{-2.7}$, $m = 0.61$, $k = 0.85$ for Model III B.

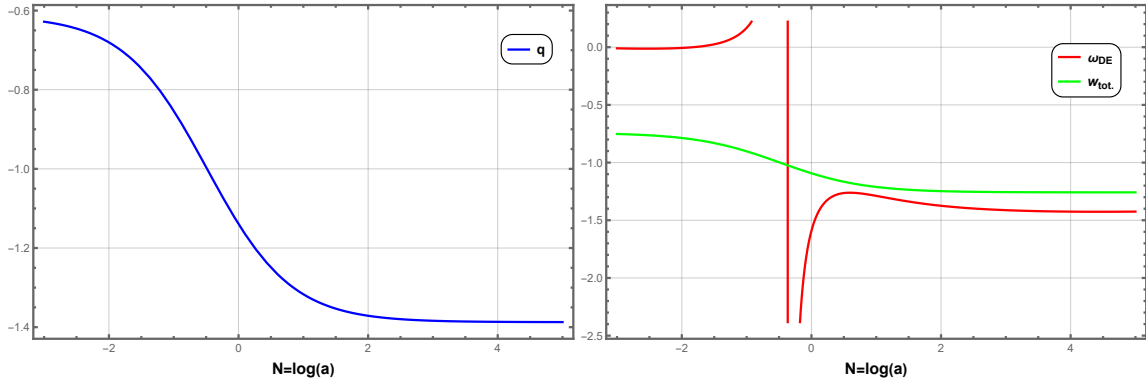


Figure 8: Deceleration and EoS parameter of Model III B. The initial conditions $X = -10^{-1.3}$, $Y = 0.089$, $Z = 0.02 \times 10^{-2}$, $V = 0.2 \times 10^{-1.5}$, $W = 0.021 \times 10^{-2.7}$, $m = 0.61$, $k = 0.85$.

The evolution of density parameters $\Omega_r, \Omega_m, \Omega_{DE}$ has been presented in Fig. 7. The vertical dashed line represents the present time at which the values of $\Omega_{DE} \approx 0.7$ and $\Omega_m \approx 0.3$. At the early epoch, we can see that the evolution curve for Ω_r is dominating the other two curves, but it will go on decreasing from the early to the late time of cosmic evolution. The deceleration parameter q (left panel) and EoS parameters in redshift $N = -\log(1+z)$ have been given in Fig. 8. Currently, the value of the deceleration parameter is obtained as $q_0 = -1.14$, which agrees with the range provided in Ref. [57]. The present value of the DE EoS parameter has been obtained as $\omega_{DE} = -1.61$ and is approximately the same as in Ref. [56].

IV. CONCLUSION

We have presented two cosmological models of the Universe in the Gauss-Bonnet teleparallel formalism through the approach of dynamical system analysis. The general dynamical system depending on the form of $f(T, T_G)$, has been presented in Eq. (27). This dynamical system is capable of deriving critical points explaining the early and late times of cosmic evolution for the mixed power law and the separated forms of the power law. The dimensionless variables are presented in (22) to obtain an autonomous dynamical system.

The dynamical system for the mixed power law model is presented in Eq. (32). The critical points and the existence condition for Model III A are presented in Table I. To study the stability of critical points at different phases of Universe evolution, the value of the deceleration parameter, $\omega_{tot}, \omega_{DE}$, are presented in Table II. From this, it has been observed that the critical points representing the DE-dominated era are showing stable behavior, while the critical points representing the radiation, cold dark matter-dominated eras are unstable. The exact cosmological solutions

and the evolution equations at each critical point are presented in Table III. The study of the behavior of phase space trajectories supports the stability conditions and can be analyzed from the 2-D phase space plot presented in Fig. 1. The evolution plots for the density parameter for Model III A are presented in Fig. 3, which show the value of $\Omega_{DE} \approx 0.7$ and $\Omega_m \approx 0.3$ at the present time. The plots for ω_{DE} , ω_{tot} , and the deceleration parameter are also presented in Fig. 4, which show compatibility with the current observation study.

The second model that we studied is the sum of separated power law and is presented in Subsection III B; the dynamical system for this model is presented in Eq. (35). This model can also describe different phases of the Universe's evolution with more critical points than in Model III A. Table V presents the critical points and existing conditions. Although the dynamical variable λ shows dependency on the other variables in Model III A, it plays a crucial role in identifying different phases of Universe evolution in Model III B analysis. We have categorized the critical points depending on $\lambda = 8, \frac{9}{2}$ and depending on X, Y, Z for the radiation-dominated era, the cold-dark matter-dominated era, and the DE, respectively. The stability conditions and the eigenvalues of the Jacobian matrix are presented in Table VI and Table VIII, which play an important role in analyzing the stability of critical points. In this case, the standard density parameters at each critical point and the evolution equation, along with the exact cosmological solutions, are presented in Table VII. The analysis of the behaviour of phase space trajectories supports the stability criteria. It may be evaluated using the 2-D phase space plot shown in Fig. 5. The evolution graphs for the density parameter for the second model are shown in Fig. 7, with current values of $\Omega_{DE} \approx 0.7$ and $\Omega_m \approx 0.3$. The graphs for ω_{DE} , ω_{tot} and the deceleration parameter are shown in Fig. 8. Each model has a phase space trajectory drawn in 3D space (see Fig. 2, Fig.6). The trajectory transitions from matter-dominated (unstable) to dark energy-dominated (stable) phases. From this study, it has analyzed that the cosmological viable models, the mixed power law, and the sum of separated power law models play an important role in the study of the Universe evolution and show compatibility with the current observational study; the more work can be done in this direction.

APPENDIX

$$r = \sqrt{-\left(x_1(v_1 - 8x_1 - 1)\left(-v_1(9x_1 + 2) + 2v_1^2 + 8x_1^2 + x_1\right)\right)},$$

$$s = \sqrt{x_4(8mx_4 - 1)(2m(6x_4 + 1)^2 - 17x_4 - 2)}. \quad (37)$$

and,

$$\tau_2 = \sqrt{X_2^2 \left(((m-1)(V_2-1) + 2(5-6m)X_2)^2 - 16(m_4-1)(V_2-1)X_2 \right)},$$

$$\tau_5 = \sqrt{(12k^2m - 4km + 2k^2)^2 - 4(72k^4m + 24k^3m - 120k^4)},$$

$$\tau_7 = \sqrt{\left(-2mX_7W_7 + 12mX_7^2 + 2X_7W_7 - 6X_7^2\right)^2 - 4\left(12X_7X_7^3W_7 + 72mX_7^4 - 12X_7^3W_7 - 72X_7^4\right)},$$

$$\tau_9 = \sqrt{k^2 \left(Z_9^2(2-5k)^2 + Z_9(22k^2 - 24k + 8) + (k-2)^2 \right)},$$

$$\tau_{10} = \frac{\sqrt{X_{10}^2(Y_{10} - 2X_{10})^2 \left(2Y_{10}(6(1-2m)X_{10} + m - 1) + (6(2m-1)X_{10} + m - 1)^2 + Y_{10}^2 \right)}}{2X_{10} - Y_{10}}. \quad (38)$$

ACKNOWLEDGEMENTS

SAK acknowledges the financial support provided by University Grants Commission (UGC) through Senior Research Fellowship (UGC Ref. No.: 191620205335), and S.V.L. acknowledges the financial support provided by the University Grants Commission (UGC) through Senior Research Fellowship (UGC Ref. No.: 191620116597) to carry

out the research work. BM acknowledges IUCAA, Pune, India, for hospitality and support during an academic visit where a part of this work has been accomplished.

REFERENCES

-
- [1] **Supernova Search Team** Collaboration, A. G. Riess *et al.*, "Observational evidence from supernovae for an accelerating universe and a cosmological constant," *Astron. J.* **116** (1998) 1009–1038, [arXiv:astro-ph/9805201](#).
- [2] **Supernova Cosmology Project** Collaboration, S. Perlmutter *et al.*, "Measurements of Ω and Λ from 42 high redshift supernovae," *Astrophys. J.* **517** (1999) 565–586, [arXiv:astro-ph/9812133](#).
- [3] E. J. Copeland, M. Sami, and S. Tsujikawa, "Dynamics of dark energy," *Int. J. Mod. Phys. D* **15** (2006) 1753–1936, [arXiv:hep-th/0603057](#).
- [4] K. Bamba, S. Capozziello, S. Nojiri, and S. D. Odintsov, "Dark energy cosmology: the equivalent description via different theoretical models and cosmography tests," *Astrophys. Space Sci.* **342** (2012) 155–228, [arXiv:1205.3421 \[gr-qc\]](#).
- [5] L. Baudis, "Dark matter detection," *J. Phys. G* **43** (2016) no. 4, 044001.
- [6] G. Bertone, D. Hooper, and J. Silk, "Particle dark matter: Evidence, candidates and constraints," *Phys. Rept.* **405** (2005) 279–390, [arXiv:hep-ph/0404175](#).
- [7] T. Kobayashi, M. Yamaguchi, and J. Yokoyama, "Generalized G-Inflation: Inflation with the Most General Second-Order Field Equations," *Progr. Theor. Phys.* **126** (2011) no. 3, 511–529, [arXiv:1105.5723 \[hep-th\]](#).
- [8] C. Misner, K. Thorne, and J. Wheeler, *Gravitation*. No. pt. 3 in *Gravitation*. W. H. Freeman, 1973. <https://books.google.com.mt/books?id=w4Gigq3tY1kC>.
- [9] M. Nakahara, *Geometry, Topology and Physics, Second Edition*. Graduate student series in physics. Taylor & Francis, 2003. <https://books.google.com.mt/books?id=cH-XQB0Ex5wC>.
- [10] K. Hayashi and T. Shirafuji, "New General Relativity," *Phys. Rev. D* **19** (1979) 3524–3553. [Addendum: *Phys.Rev.D* **24**, 3312–3314 (1982)].
- [11] R. Aldrovandi and J. G. Pereira, *Teleparallel Gravity: An Introduction*. Springer, 2013.
- [12] R. Weitzenböck, 'Invariantentheorie'. Noordhoff, Gronningen, 1923.
- [13] S. Bahamonde *et al.*, "Teleparallel gravity: from theory to cosmology," *Rep. Prog. Phys.* **86** (2023) 207pp, [arXiv:2106.13793 \[gr-qc\]](#).
- [14] T. Clifton, P. G. Ferreira, A. Padilla, and C. Skordis, "Modified Gravity and Cosmology," *Phys. Rept.* **513** (2012) 1–189, [arXiv:1106.2476 \[astro-ph.CO\]](#).
- [15] Y.-F. Cai, S. Capozziello, M. De Laurentis, and E. N. Saridakis, " $f(T)$ teleparallel gravity and cosmology," *Rept. Prog. Phys.* **79** (2016) no. 10, 106901, [arXiv:1511.07586 \[gr-qc\]](#).
- [16] M. Krssak, R. J. van den Hoogen, J. G. Pereira, C. G. Böhrmer, and A. A. Coley, "Teleparallel theories of gravity: illuminating a fully invariant approach," *Class. Quant. Grav.* **36** (2019) no. 18, 183001, [arXiv:1810.12932 \[gr-qc\]](#).
- [17] S. Bahamonde, C. G. Böhrmer, and M. Wright, "Modified teleparallel theories of gravity," *Phys. Rev. D* **92** (2015) no. 10, 104042, [arXiv:1508.05120 \[gr-qc\]](#).
- [18] G. Farrugia and J. Levi Said, "Stability of the flat FLRW metric in $f(T)$ gravity," *Phys. Rev. D* **94** (2016) no. 12, 124054, [arXiv:1701.00134 \[gr-qc\]](#).
- [19] T. P. Sotiriou and V. Faraoni, " $f(R)$ Theories Of Gravity," *Rev. Mod. Phys.* **82** (2010) 451–497, [arXiv:0805.1726 \[gr-qc\]](#).
- [20] V. Faraoni, " $f(R)$ gravity: Successes and challenges," in *18th SIGRAV Conference*. 10, 2008. [arXiv:0810.2602 \[gr-qc\]](#).
- [21] S. Capozziello and M. De Laurentis, "Extended Theories of Gravity," *Phys. Rept.* **509** (2011) 167–321, [arXiv:1108.6266 \[gr-qc\]](#).
- [22] J. T. Wheeler, "Symmetric solutions to the gauss-bonnet extended einstein equations," *Nucl. Phys. B* **268** (1986) no. 3, 737–746.
- [23] A. De Felice and S. Tsujikawa, "Solar system constraints on $f(G)$ gravity models," *Phys. Rev. D* **80** (2009) no. 6, 063516, [arXiv:0907.1830 \[hep-th\]](#).
- [24] A. Jawad, S. Chattopadhyay, and A. Pasqua, "Reconstruction of $f(G)$ gravity with the new agegraphic dark-energy model," *Eur. Phys. J. P.* **128** (2013) no. 8, 88.
- [25] R. Ferraro and F. Fiorini, "Modified teleparallel gravity: Inflation without inflaton," *Phys. Rev. D* **75** (2007) 084031, [arXiv:gr-qc/0610067 \[gr-qc\]](#).
- [26] R. Ferraro and F. Fiorini, "On Born-Infeld Gravity in Weitzenböck spacetime," *Phys. Rev. D* **78** (2008) 124019, [arXiv:0812.1981 \[gr-qc\]](#).

- [27] G. R. Bengochea and R. Ferraro, “Dark torsion as the cosmic speed-up,” *Phys. Rev. D* **79** (2009) 124019, [arXiv:0812.1205 \[astro-ph\]](#).
- [28] E. V. Linder, “Einstein’s Other Gravity and the Acceleration of the Universe,” *Phys. Rev. D* **81** (2010) 127301, [arXiv:1005.3039 \[astro-ph.CO\]](#). [Erratum: *Phys.Rev.D* 82, 109902 (2010)].
- [29] S.-H. Chen, J. B. Dent, S. Dutta, and E. N. Saridakis, “Cosmological perturbations in $f(T)$ gravity,” *Phys. Rev. D* **83** (2011) 023508, [arXiv:1008.1250 \[astro-ph.CO\]](#).
- [30] S. Bahamonde, K. Flathmann, and C. Pfeifer, “Photon sphere and perihelion shift in weak $f(T)$ gravity,” *Phys. Rev. D* **100** (2019) no. 8, 084064, [arXiv:1907.10858 \[gr-qc\]](#).
- [31] G. A. R. Franco, C. Escamilla-Rivera, and J. Levi Said, “Stability analysis for cosmological models in $f(T, B)$ gravity,” *Eur. Phys. J. C* **80** (2020) no. 7, 677, [arXiv:2005.14191 \[gr-qc\]](#).
- [32] G. Kofinas and E. N. Saridakis, “Teleparallel equivalent of Gauss-Bonnet gravity and its modifications,” *Phys. Rev. D* **90** (2014) 084044, [arXiv:1404.2249 \[gr-qc\]](#).
- [33] S. Capozziello, M. De Laurentis, and K. F. Dialektopoulos, “Noether symmetries in Gauss–Bonnet-teleparallel cosmology,” *Eur. Phys. J. C* **76** (2016) no. 11, 629, [arXiv:1609.09289 \[gr-qc\]](#).
- [34] G. A. Rave-Franco, C. Escamilla-Rivera, and J. L. Said, “Dynamical complexity of the teleparallel gravity cosmology,” *Phys. Rev. D* **103** (2021) 084017, [arXiv:2101.06347 \[gr-qc\]](#).
- [35] M. Hohmann, L. Järv, and U. Ualikhanova, “Dynamical systems approach and generic properties of $f(T)$ cosmology,” *Phys. Rev. D* **96** (2017) 043508, [arXiv:1706.02376 \[gr-qc\]](#).
- [36] G. Kofinas and E. N. Saridakis, “Cosmological applications of $F(T, T_G)$ gravity,” *Phys. Rev. D* **90** (2014) 084045, [arXiv:1408.0107 \[gr-qc\]](#).
- [37] J. Dutta, W. Khyllep, and H. Zonunmawia, “Cosmological dynamics of the general non-canonical scalar field models,” *Eur. Phys. J. C* **79** (2019) 1–14, [arXiv:1812.07836 \[gr-qc\]](#).
- [38] L. K. Duchaniya, S. A. Kadam, J. L. Said, and B. Mishra, “Dynamical systems analysis in $f(T, \phi)$ gravity,” *Eur. Phys. J. C* **83** (2023) no. 1, 27, [arXiv:2209.03414 \[gr-qc\]](#).
- [39] L. K. Duchaniya, S. V. Lohakare, B. Mishra, and S. K. Tripathy, “Dynamical stability analysis of accelerating $f(T)$ gravity models,” *Eur. Phys. J. C* **82** (2022) no. 5, 448, [arXiv:2202.08150 \[gr-qc\]](#).
- [40] G. Kofinas, G. Leon, and E. N. Saridakis, “Dynamical behavior in $f(T, T_G)$ cosmology,” *Class. Quant. Grav.* **31** (2014) 175011, [arXiv:1404.7100 \[gr-qc\]](#).
- [41] S. A. Kadam, B. Mishra, and J. Said Levi, “Teleparallel scalar-tensor gravity through cosmological dynamical systems,” *Eur. Phys. J. C* **82** (2022) no. 8, 680, [arXiv:2205.04231 \[gr-qc\]](#).
- [42] S. A. Kadam, B. Mishra, and J. L. Said, “Noether symmetries in $f(T, TG)$ cosmology,” *Physica Scripta* **98** (2023) no. 4, 045017, [arXiv:2210.06166 \[gr-qc\]](#).
- [43] A. de la Cruz-Dombriz, G. Farrugia, J. L. Said, and D. Sáez-Chillón Gómez, “Cosmological bouncing solutions in extended teleparallel gravity theories,” *Phys. Rev. D* **97** (2018) no. 10, 104040, [arXiv:1801.10085 \[gr-qc\]](#).
- [44] A. de la Cruz-Dombriz, G. Farrugia, J. L. Said, and D. Saez-Gomez, “Cosmological reconstructed solutions in extended teleparallel gravity theories with a teleparallel Gauss–Bonnet term,” *Class. Quant. Grav.* **34** (2017) no. 23, 235011, [arXiv:1705.03867 \[gr-qc\]](#).
- [45] S. V. Lohakare, B. Mishra, S. K. Maurya, and K. N. Singh, “Analyzing the geometrical and dynamical parameters of modified teleparallel-gauss–bonnet model,” *Phys. Dark Univ.* **39** (2023) 101164, [arXiv:2209.13197 \[gr-qc\]](#).
- [46] G. Otorola, “Cosmological dynamics of tachyonic teleparallel dark energy,” *Phys. Rev. D* **88** (2013) 063505, [arXiv:1305.5896 \[gr-qc\]](#).
- [47] S. Narawade, L. Pati, B. Mishra, and S. Tripathy, “Dynamical system analysis for accelerating models in non-metricity $f(Q)$ gravity,” *Phys. Dark Univ.* **36** (2022) 101020, [arXiv:2203.14121 \[gr-qc\]](#).
- [48] A. S. Agrawal, B. Mishra, and P. K. Agrawal, “Matter bounce scenario in extended symmetric teleparallel gravity,” *Eur. Phys. J. C* **83** (2023) no. 2, , [arXiv:2206.02783 \[gr-qc\]](#).
- [49] S. Chandrasekhar, “The Mathematical Theory of Black Holes,” *Fundam. Theor. Phys.* **9** (1984) 5–26.
- [50] M. Krššák and E. N. Saridakis, “The covariant formulation of $f(T)$ gravity,” *Class. Quant. Grav.* **33** (2016) no. 11, 115009, [arXiv:1510.08432 \[gr-qc\]](#).
- [51] M. Zubair and A. Jawad, “Generalized Second Law of Thermodynamics in $f(T, T_G)$ gravity,” *Astrophys. Space Sci.* **360** (2015) 11, [arXiv:1505.07337 \[gr-qc\]](#).
- [52] S. Bahamonde and C. G. Böhrer, “Modified teleparallel theories of gravity: Gauss–Bonnet and trace extensions,” *Eur. Phys. J. C* **76** (2016) no. 10, 578, [arXiv:1606.05557 \[gr-qc\]](#).
- [53] N. Tamanini and C. G. Boehmer, “Good and bad tetrads in $f(T)$ gravity,” *Phys. Rev. D* **86** (2012) 044009, [arXiv:1204.4593 \[gr-qc\]](#).
- [54] S. D. Odintsov and V. K. Oikonomou, “Dynamical systems perspective of cosmological finite-time singularities in $f(R)$ gravity and interacting multifluid cosmology,” *Phys. Rev. D* **98** (2018) 024013, [arXiv:1806.07295 \[gr-qc\]](#).

- [55] C. Gruber and O. Luongo, “Cosmographic analysis of the equation of state of the universe through padé approximations,” *Phys. Rev. D* **89** (2014) 103506, [arXiv:1309.3215 \[gr-qc\]](#).
- [56] G. Hinshaw *et al.*, “Nine-year Wilkinson Microwave Anisotropy Probe (WMAP) observations: cosmological parameter results,” *Astro. J. Supp. Ser.* **208** (2013) 19, [arXiv:1212.5226 \[astro-ph\]](#).
- [57] S. M. Feeney, D. J. Mortlock, and N. Dalmasso, “Clarifying the Hubble constant tension with a Bayesian hierarchical model of the local distance ladder,” *Month. Noti. Roy. Astro. Soc.* **476** (2018) no. 3, 3861–3882, [arXiv:1707.00007 \[astro-ph\]](#).